2014 5th IEEE RAS & EMBS International Conference on
Biomedical Robotics and Biomechatronics (BioRob)
August 12-15, 2014. São Paulo, Brazil

Kinematic Instability in Concentric-tube Robots: Modeling and Analysis

Ran Xu[†], S. Farokh Atashzar[†] and Rajni V. Patel

Abstract— **In this paper the issue of kinematic instability for concentric tube robots is studied when the following two conditions are considered: (a) the robot consists of more than two concentric tubes, and (b) the tubes consist of straight sections followed by curved sections. In this paper, we use the term "kinematic instability" when the tip position of robot in the Cartesian domain jumps from one equilibrium point to another while having a constant joint space configuration. This implies that in unstable configurations, the "forward kinematics" of the robot will have multiple solutions for one set of joint space variables. In this paper a novel framework is proposed that can calculate the stability condition for the robots consisting of multiple tubes with straight sections without solving the nonlinear ordinary differential equations. The resulting conditions restrict the pre-curvatures and length of the tubes, as a design factor, to guarantee kinematic stability within the whole workspace of the robot.**

I. INTRODUCTION

Concentric-tube robots have attracted a great deal of interest during last five years due to the high dexterity and articulation that they can provide while having light weight, small diameter and hollow-shaft design. The aforementioned features make concentric-tube robots as a potential future for delicate surgical procedures where dexterity is a need and the surgical environment is sensitive. In the literature, several surgical procedures have been proposed as applications that can take advantage of the unique physics of this robot, such as beating-heart tissue removal procedures [1], patent foramen ovale closure [2], and intracerebral hemorrhage evacuation [3]. Because of the specific features of the kinematic chain and the different flow of motion/force/energy in concentric-tube robots, the conventional theory for classical robotics is not applicable. As a result, in the literature, several challenges in kinematic modeling for this type of robots, such as those resulting from bending, torsion [4] [5], friction [6], and external loading [7] have been considered. The complex physics of this robot that involves several mechanical couplings makes the computational cost high. Consequently, new quasi-analytical techniques are being developed to deal with such computational difficulties [8]. In addition to the modeling challenges, control and navigation of this robot has some unique features that differ from conventional control techniques in classical robotics. Therefore, currently several research teams are working on addressing the fundamental control challenges for this robot namely: motion planning [9], inverse-kinematics-based and Jacobian-based position control [4] [10] [11], force disturbance rejection during targeting [12], compliance tuning in dealing with sensitive areas [13].

R. Xu, and S.F. Atashzar contributed equally to the work described in this paper. The authors are with Canadian Surgical Technologies and Advanced Robotics (CSTAR), Lawson Health Research Institute, London, Canada, and with the Dept. of Electrical and Computer Engineering, Western University, London, Canada. R.V. Patel is also with the Department of Surgery, Western University (emails: rxu25@uwo.ca, satashza@uwo.ca, rvpatel@uwo.ca). Partial financial support was provided by the following grants awarded to R.V. Patel: the Natural Sciences and Engineering Research Council (NSERC) of Canada, grant RGPIN1345, the NSERC Collaborative Research and Training Experience (CREATE) program grant #371322-2009 on Computer-Assisted Medical Interventions (CAMI), and the Canada Research Chairs Program and a Canada Foundation for Innovation grant. Partial financial support for R. Xu was also provided by a postgraduate scholarship from the Peoples Republic of China.

The focus of this paper is a specific phenomenon, which exists in concentric-tube robots namely kinematic instability or the "snapping" problem. Based on the related literature [4] [5] [14], kinematic instability is when the forward kinematics solution of the concentric-tube robots loses the uniqueness; as a result the robot will jump quickly from one equilibrium position (with higher potential energy) to another equilibrium point (with lower potential energy). This fast and unexpected motion of the tip position cannot be controlled using joint variables; therefore, it can lead to unsafe interactions between the robot and the operational environment. Appropriately addressing the issue is vital for surgical applications (such as in neurosurgery).

It should be mentioned that in the literature the stability condition for a two-tube robot is derived while, to the best knowledge of the authors, extension to more complex cases (such as robots with more than two-tube interactions) have not been addressed yet. In this paper the main focus is developing stability conditions for use in designing concentric tube robots under the following two considerations: (a) the number of the tubes can be more than two, (b) the tubes can have straight parts before leading to the curvature. Using the technique proposed in this paper, stability conditions for complex concentric tube robots can be derived.

II. KINEMATIC STABILITY CONDITION FOR TWO CONCENTRIC-TUBES

In this section, a framework is implemented to find the kinematic stability conditions for two-tube robots with and without straight portions; the former result (without considering the straight parts) is compared to the results presented in the literature for two tubes.

A. Kinematic Model for Concentric-tube Robots

In this paper, a widely-used torsionally-complaint kinematics model, discussed in [4], is utilized for analysis of the instability problem. The model is shown in (1), in which, α_m represents the rotational angle difference between the first and m^{th} tube, and the total number of tubes in the robot is denoted as p. In addition, torsion (around z) and bending curvature (around x and y) are denoted by u_{mz} and $u_m|_{x,y}$, respectively. x, y and z are the axes of the tube's material coordinate frame [4]. Pre-curvatures of the tubes are denoted as $\hat{u}_{mx}$, $\hat{u}_{my}$ and $\hat{u}_{mz}$ ($\hat{u}_{mz}$ is assumed to be zero [4]). K_n is a diagonal matrix consisting of the tubes' stiffnesses in different directions namely: k_{mx} for the x direction, k_{my} for the y direction, and k_{mz} for the z direction. Note that, in the literature [4], it has been assumed that the stiffness of the tubes are isotropic in x and y directions ($k_{mx} = k_{my} = k_{mxy}$). In (1), s is the length variable. Note that the tube pre-curvatures, the tube stiffness, the angle differences, and the curvatures are functions of s which has been omitted in (1) for simplicity.

$$
\begin{aligned}
u_{mz} &= (-1/k_{1z})(k_{2z}u_{2z} + \cdots + k_{pz}u_{pz}) \\
\dot{u}_{mz} &= \frac{du_{mz}}{ds} = (k_{mxy}/k_{mz})(u_{mx}\hat{u}_{my} - u_{my}\hat{u}_{mx}) \\
u_m|_{x,y} &= \Big(\Big(\sum_{n=1}^{p} K_n\Big)^{-1} R_z^T(\alpha_m)\Big(\sum_{n=1}^{p} R_z(\alpha_n)K_n\hat{u}_n\Big)\Big)\Big|_{x,y} \\
\dot{\alpha}_m &= \frac{d\alpha_m}{ds} = u_{mz} - u_{1z}, \qquad m = 2, ..., p
\end{aligned} \tag{1}
$$

Using the above-mentioned model, to analyze the instability phenomenon, the conditions for uniqueness of the forward kinematics solution should be calculated. The complex physics of interactions between the tubes makes the resulting equations a set of nonlinear ordinary differential equations (ODEs) with boundary conditions.

B. Kinematic Stability Condition for Two-tube Robots Without Straight Parts

To obtain the stability condition, in this part, a linearization framework (along the whole body of the robot) is proposed that calculates the linearized model of the system when the linearization point is considered as a new variable. The linearized behavior of the system is then analyzed using the standard techniques for dealing with a set of linear ODEs with boundary-conditions. Finally the uniqueness condition is determined, which guarantees kinematic stability.

It should be mentioned that the behavior of the linearized system can be a good approximation of the nonlinear system only in a very small neighborhood around the linearization point. Also considering the fact that in concentric-tube robots, the kinematics variables can change significantly along the tubes, the linearization can be inaccurate if it is performed with respect to only a few points along the robot. In order to address this problem, first the kinematics model is linearized with respect to the linearization variables ($q_m, m = 2, ..., q$) which corresponds to the angle differences between the tubes. The result of this linearization is a set of ODEs which can behave differently when different values for the linearization variables (q_m) are considered. Then, the behavior of the linearized system is analyzed, and finally the general uniqueness/stability condition is achieved, which is valid for all possible q_m. This means that if the stability condition is satisfied then the solution of the set of ODEs will be unique, regardless of the q_m value.

It can be seen in (1) that $\dot{\alpha}_m$ is already given by a linear equation. $\dot{u}_{mz}$ is a nonlinear function of α_m, which needs to be linearized around (q_m). Assuming that all tubes have constant pre-curvatures and they are planar tubes, the linearized set of ODEs can be achieved as follows:

$$
\begin{aligned}
\dot{u}^*_{mz} &= \dot{u}_{mz}\Big|_{\alpha_2=q_2,...,\alpha_p=q_p} \\
&\quad + \sum_{m=2}^{p} \frac{d\dot{u}_{mz}}{d\alpha_m}\Big|_{\alpha_2=q_2,...,\alpha_p=q_p}(\alpha_m - q_m) \\
\dot{\alpha}^*_m &= \dot{\alpha}_m, \quad m = 2, ..., p
\end{aligned} \tag{2}
$$

where, $\dot{u}^*_{mz}$ and $\dot{\alpha}^*_m$ are linearized version of $\dot{u}_{mz}$ and $\dot{\alpha}_m$ in (1). For two tubes, since there is only q_2 in the equations (which we set to q in this section), the explicit equations are:

$$
\begin{aligned}
\dot{u}^*_{2z} &= \frac{(1+v)k_1\|\hat{u}_1\|\|\hat{u}_2\|(-\cos(q)q + \cos(q)\alpha^*_2 + \sin(q))}{k_1 + k_2} \\
\dot{\alpha}^*_2 &= \frac{(k_1+k_2)u^*_{2z}}{k_1}, q \in \{0, 2\pi\}
\end{aligned} \tag{3}
$$

In (3) $k_n = k_{nxy}; 1 + v = k_{nxy}/k_{nz}$ $(n = 1, 2)$. The general solutions to these equations are:

$$
\begin{aligned}
u^*_{2z}(s) &= c_1 e^{s\sqrt{\cos(q)r}} + c_2 e^{-s\sqrt{\cos(q)r}} \\
\alpha^*_2(s) &= \frac{(k_1+k_2)(-c_1 e^{s\sqrt{\cos(q)r}} + c_2 e^{-s\sqrt{\cos(q)r}})}{k_1\sqrt{\cos(q)r}} + \epsilon
\end{aligned} \tag{4}
$$

where,

$$
r = (1+v)\|\hat{u}_1\|\|\hat{u}_2\| \tag{5}
$$

In this paper, $\| * \|$ denotes the Euclidean norm of a vector or the magnitude of a complex number. In (4), s is the length variable. ϵ is the trivial part of the solution, which will be discussed following equation (7). The constant values c_1 and c_2 are obtained by applying boundary conditions to the solutions, which are: $u^*_{2z}(L) = 0, \alpha^*_2(0) = \theta$, where L is the length of the curved section of the robot and θ is the angle difference between the two tubes at the proximal end [4]. After applying the boundary conditions, we have:

$$
E_2 \begin{bmatrix} c_1 & c_2 \end{bmatrix}^T + \begin{bmatrix} 0 & \epsilon \end{bmatrix}^T = \begin{bmatrix} 0 & \theta \end{bmatrix}^T \tag{6}
$$

where:

$$
E_2 = \begin{bmatrix} e^{L\sqrt{\cos(q)r}} & e^{-L\sqrt{\cos(q)r}} \\ \frac{k_1+k_2}{k_1(\sqrt{\cos(q)r})} & -\frac{k_1+k_2}{k_1(\sqrt{\cos(q)r})} \end{bmatrix} \tag{7}
$$

Consequently, the uniqueness of the robot kinematics is equal to the uniqueness of the solution for c_1 and c_2. This means that the coefficient matrix (E_2) should be non-singular to make the robot stable. It can be seen that ϵ is not multiplied by any constant variables (c_1, c_2), so the value of ϵ cannot change any part of E_2. In other words, ϵ has no effect on stability. In order to investigate the stability condition of the kinematics independently of q, the determinant of the coefficient matrix E_2 is needed as given below:

$$
D(E_2) = \frac{(k_1+k_2)(e^{L\sqrt{\cos(q)r}} + e^{-L\sqrt{\cos(q)r}})}{k_1(\sqrt{\cos(q)r})} \tag{8}
$$

It can be seen that if $q \leq \pi/2$ or $q \geq 3\pi/2$, then the determinant, $D(E_2)$, is non-negative and the kinematics has a unique solution. Therefore to find the stability condition, q should be considered as: $\pi/2 < q < 3\pi/2$, in which case, the determinant can be zero implying that the kinematics could be unstable. Consequently, considering $\pi/2 < q < 3\pi/2$, the determinant of E_2 can be simplified as follows:

$$D(E_2) = 2\frac{(k_1+k_2)\cos(L\sqrt{-\cos(q)r})}{k_1(\sqrt{-\cos(q)r})}, q \in \{\pi/2, 3\pi/2\} \tag{9}$$

In order to guarantee kinematic stability, the determinant $D(E_2)$ should not be equal to zero. Consequently, the stability condition can be satisfied as follows:

$$L\sqrt{r}\sqrt{-\cos(q)} \neq (1/2+N)\pi \tag{10}$$

where N is an integer number. Since we have $\pi/2 < q < 3\pi/2$, it is true to say that $\sqrt{-\cos(q)}$ is a real scalar and is bounded by unity. Consequently, the stability condition for all possible q can be stated as follows:

$$L\sqrt{r} < \pi/2 \tag{11}$$

The achieved result is the same as the result that has been derived directly from the nonlinear equations [4]. This supports the effectiveness of the proposed technique. Since the method can be extended for more than two tubes, it can be modified to address the general problem.

C. Including Straight Parts

The stability condition developed in the previous section assumes that the two tubes have a non-zero curvature along the whole body. This assumption is not always valid since in many applications, the tubes have a straight part before the curvature starts. In fact the inner tube usually has a straight section, extending out of the outer tube for translational motion. The straight part changes the energy function of the system and can therefore change the stability condition for the kinematics. As the first step, in this section the formulations for two tubes (which is a simpler case) are derived and in the next section they will be extended for multiple tubes. The kinematic instability in concentric-tube robots is caused by torsional energy stored in the tubes. Additional solutions to the forward kinematics may appear because of the straight section since the maximum torsion occurs within that part. In order to mathematically show the effect of the straight section on kinematic stability, the boundary condition for the system should be tuned depending on the straight part as follows:

$$u^*_{2z}(L) = 0, \alpha^*_2(0) - l_2 u^*_{2z}(0) + l_1 u^*_{1z}(0) = \theta \tag{12}$$

where l_n $(n = 1, 2)$ represents the length of the straight portion for the n^{th} tube. Consequently, the determinant of the coefficient matrix ($D(E^l_2)$) will be:

$$-(k_2 l_1 + k_1 l_2)\tanh(L\sqrt{\cos(q)r})\sqrt{\cos(q)r} - (k_1+k_2) \tag{13}$$

As a result, the kinematics will have multiple solutions if (13) equals to zero.

Knowing that $\tanh(*) = -i\tan(i*)$, where i is $\sqrt{-1}$ and considering $D(E^l_2)$ = 0, we will have:

$$Li\sqrt{\cos(q)r} = \arctan\left(\frac{k_1+k_2}{(k_1 l_2 + k_2 l_1)i\sqrt{\cos(q)r}}\right) \tag{14}$$

Taking the Euclidean norm on both sides:

$$\left\|Li\sqrt{\cos(q)r}\right\| = \left\|\arctan\left(\frac{k_1+k_2}{(k_1 l_2 + k_2 l_1)i\sqrt{\cos(q)r}}\right)\right\| \tag{15}$$

Considering (15), and also $\|\arctan(*)\| \geq \arctan(\|*\|)$, the following can be developed:

$$L\left\|i\sqrt{\cos(q)r}\right\| \geq \arctan\left(\frac{k_1+k_2}{(k_1 l_2 + k_2 l_1)\left\|i\sqrt{\cos(q)r}\right\|}\right) \tag{16}$$

As can be seen in (5), r is a positive real number; as a result we have: $\sqrt{r} \geq \left\|\sqrt{\cos(q)r}\right\| = \left\|i\sqrt{\cos(q)r}\right\|$. Accordingly, (16) will result in the following:

$$L\sqrt{r} \geq \arctan\left(\frac{k_1+k_2}{(k_1 l_2 + k_2 l_1)\sqrt{r}}\right) \tag{17}$$

Consequently, when the kinematics are unstable ($D(E^l_2) = 0$), the tube parameters will satisfy the relation shown in (17). In other words, if the tube parameters are chosen such that (17) is never satisfied, then kinematic stability will be guaranteed. As a result, one stability condition for two-tube interaction considering the effects of the straight sections is as follows:

$$L\sqrt{r} < \arctan\left(\frac{k_1+k_2}{(k_1 l_2 + k_2 l_1)\sqrt{r}}\right) \tag{18}$$

This stability condition exhibits the effect of the straight section. It can be seen that, for the robot having the same curved sections $\sqrt{r}$, the longer the straight part, the greater the chances of instability. When $l_1, l_2 \to 0$ the proposed condition reduces to the original condition given in (11) since $\arctan\left(\frac{k_1+k_2}{(k_1 l_2+k_2 l_1)\sqrt{r}}\right) \to \pi/2$.

III. Kinematic Stability Condition for Three or Multiple Concentric-tubes

In this section, the stability conditions are extended to three-tube robots and finally to multi-tube robots.

A. Three-tube Robots without Straight Parts

It should be noted that because of significant mathematical complexity, it is neither efficient nor practical to calculate an explicit solution for the kinematics model when the robot has more than two tubes. Even if a solution can be obtained, the mathematical complexity makes it almost impossible to analyze the solution properly and have a stability condition that can be used in designing robots. Consequently, an indirect technique is proposed in the rest of this section, which can calculate a stability condition with no need for an explicit solution. For this purpose, the linearized model for the three-tube robot (calculated from (2) when $q = 3$) can be written as a set of linear first-order ODEs in the form:

$$\dot{x} = \frac{dx}{ds} = Ax + B \tag{19}$$

where $x = [u^*_{2z}, u^*_{3z}, \alpha^*_2, \alpha^*_3]$. Considering (2) and (19), after some algebraic manipulations, it can be shown that for a three-tube robot, the matrix A is 4 by 4 in dimension and is always in the anti-diagonal block structure. A and B are shown as below:

$$A = \begin{bmatrix} 0 & 0 & a_{13} & a_{14} \\ 0 & 0 & a_{23} & a_{24} \\ a_{31} & a_{32} & 0 & 0 \\ a_{41} & a_{42} & 0 & 0 \end{bmatrix}, \; B = \begin{bmatrix} b_1 \\ b_2 \\ b_3 \\ b_4 \end{bmatrix} \tag{20}$$

In (20), the elements in A and B ($a_{ij}, b_j; i, j = 1, 2, 3, 4$) are dependent on some of the tubes' parameters ($\hat{u}, k, L$) and linearization variables (q_m). The general solution for this system has the following specific structure:

$$x(s) = Ve^{\Lambda s}C + \int_0^s Ve^{\Lambda(s-\tau)}V^{-1}Bd\tau \tag{21}$$

where,

$$V = \begin{bmatrix} v_{11} & -v_{11} & v_{13} & -v_{13} \\ v_{21} & -v_{21} & v_{23} & -v_{23} \\ v_{31} & v_{31} & v_{33} & v_{33} \\ 1 & 1 & 1 & 1 \end{bmatrix} \tag{22}$$

In (22), Λ is a diagonal matrix consisting of the eigenvalues ($\lambda_j; j = 1, 2, 3, 4$) of A, and V represents a matrix of its eigenvectors. It can be shown that because of its structure, the matrix A always has four distinct eigenvalues which have the following relationship: $\lambda_2 = -\lambda_1$, $\lambda_4 = -\lambda_3$. $C = V^{-1}x(0)$ is a constant vector that is to be determined. To calculate C, the boundary conditions ($u^*_{2z}(L) = 0, u^*_{3z}(L) = 0, \alpha^*_2(0) = \theta_2, \alpha^*_3(0) = \theta_3$) are applied to the general solution, which results in:

$$E_3C + x_\epsilon = [0 \;\; 0 \;\; \theta_2 \;\; \theta_3]^T \tag{23}$$

where,

$$E_3 = \begin{bmatrix} v_{11}e^{\lambda_1 L} & -v_{11}e^{\lambda_2 L} & v_{13}e^{\lambda_3 L} & -v_{13}e^{\lambda_4 L} \\ v_{21}e^{\lambda_1 L} & -v_{21}e^{\lambda_2 L} & v_{23}e^{\lambda_3 L} & -v_{23}e^{\lambda_4 L} \\ v_{31} & v_{31} & v_{33} & v_{33} \\ 1 & 1 & 1 & 1 \end{bmatrix} \tag{24}$$

and the vector x_ϵ is calculated from the integral term in (21). As discussed for equation (7), the uniqueness of these general solutions, only depends on whether the coefficient matrix E_3 is invertible or not. In other words, there is only one solution for the robot kinematics if the determinant of the coefficient matrix ($D(E_3)$) is not zero. Considering the relationship between the eigenvalues ($\lambda_2 = -\lambda_1$, $\lambda_4 = -\lambda_3$), $D(E_3)$ is calculated as follows:

$$D(E_3) = v_\epsilon(e^{-L\lambda_1} + e^{L\lambda_1})(e^{-L\lambda_3} + e^{L\lambda_3}) \tag{25}$$

where $v_\epsilon = -(v_{31} - v_{33})(v_{11}v_{23} - v_{13}v_{21})$. Note that v_ϵ equal to zero will make at least two eigenvectors of A linearly dependent (see the structure of V in (22)), which cannot be true for a 4×4 matrix having four distinct eigenvalues. Consequently, since v_ϵ cannot be zero, the robot kinematics will be stable as long as the following holds:

$$D(E_3) \neq 0 \Longleftrightarrow \lambda_j \neq \pm i\pi/2L \tag{26}$$

We can define the critical value ($\lambda^\dagger$) for the eigenvalues which makes the kinematics unstable as:

$$\lambda^\dagger = \pm i\pi/2L \tag{27}$$

Up to this point, kinematic stability is established based on the definition of the critical value ($\lambda^\dagger$) for the eigenvalues of the matrix A. In order to guarantee kinematic stability, first the eigenvalues of A should be calculated as functions of the tube parameters ($\hat{u}, k, l, L$) using the characteristic polynomial of A. Then the stability condition should be calculated in order to provide acceptable bounds for the tube parameters that prevent the eigenvalues from being equal to the critical value ($\lambda^\dagger$). However, calculating the relationship between λ_j and tube parameters by solving the characteristic equation of the system ($D(\lambda) = 0$) is not straightforward, because of the algebraic complexity. The aforementioned issue will become more complicated when the number of tubes increases. In order to address this, an indirect technique is proposed in this section, which can provide a compact sufficient stability condition that can be used in selecting tube parameters for designing concentric tube robots.

For the above-mentioned purpose, a novel inner product of the pre-curvatures of two tubes is defined:

$$[\hat{u}_m, \hat{u}_n] = r_{mn}\cos(q_{mn}) \tag{28}$$

where,

$$r_{mn} = (1 + v)\|\hat{u}_m\|\|\hat{u}_n\| \tag{29}$$

and $q_{mn} = q_m - q_n, q_{m1} = q_m$. In (28), (29) and the rest of this subsection, the subscripts $m, n = 1, 2, 3; m > n$. From the definition of the inner product in (28), the following two inequalities can be obtained:

$$\|[\hat{u}_m, \hat{u}_n]\| \leq r_{mn} \tag{30}$$

$$\left\|\sqrt{[\hat{u}_m, \hat{u}_n]}\right\| \leq \sqrt{r_{mn}} \tag{31}$$

Substituting the proposed definition (28), into the characteristic polynomial ($D(\lambda)$) results in :

$$\begin{aligned} D(\lambda) = \frac{1}{\sum_{i=1}^{3} k_i}\Big(&k_1([\hat{u}_2, \hat{u}_1] - \lambda^2)([\hat{u}_3, \hat{u}_1] - \lambda^2) \\ &+ k_2([\hat{u}_2, \hat{u}_1] - \lambda^2)([\hat{u}_3, \hat{u}_2] - \lambda^2) \\ &+ k_3([\hat{u}_3, \hat{u}_1] - \lambda^2)([\hat{u}_3, \hat{u}_2] - \lambda^2)\Big) \end{aligned} \tag{32}$$

The resulting equation provides better insight into the relationships between the tube parameters and the eigenvalues. From $D(\lambda) = 0$, it can be shown that, λ^2 always has real values. Consequently, the solutions for λ that satisfied $D(\lambda) = 0$ are either purely real or purely imaginary. Considering (32), the solution for λ^2 (that can make $D(\lambda) = 0$) will satisfy (33), and (34):

$$\min([\hat{u}_m, \hat{u}_n]) \leq \lambda_j^2 \leq \max([\hat{u}_m, \hat{u}_n]) \tag{33}$$

$$\|\lambda_j\| \leq \max\left(\left\|\sqrt{[\hat{u}_m, \hat{u}_n]}\right\|\right) \tag{34}$$

From (31) and (34), we have:

$$\|\lambda_j\| \leq \max(\sqrt{r_{mn}}) \tag{35}$$

The inequality above shows the bound of the eigenvalues according to the tube parameters. As a result, the robot kinematics will be stable over the whole workspace if the $\|\lambda^\dagger\|$ is not in this bound:

$$\max(\sqrt{r_{mn}}) < \left\|\lambda^\dagger\right\| \tag{36}$$

which can be rewritten as follows by combining with (27):

$$\max(L\sqrt{r_{mn}}) < \pi/2 \tag{37}$$

It should be noted that, since the upper bound of $\|\lambda\|$ is utilized to establish the stability condition, instead of the exact solution for $\|\lambda\|$, the result is a sufficient condition.

In other words, it is possible that the robot is stable, when using tube parameters outside the range defined in (37).

B. Three-tube Robots Including Straight Parts

In this section, the goal is to define the stability condition for three-tube robots with straight parts, in which the boundary conditions have the following form: $u_{mz}(L) = 0, \alpha_m(0) - u_{mz}(0)l_m + u_{1z}(0)l_1 = \theta_m$. Consequently, the determinant of the coefficient matrix can be obtained following a similar approach as in (25):

$$\begin{aligned} D(E_3^l) &= h_1 e^{L(\lambda_1+\lambda_3)} + h_2 e^{L(\lambda_1-\lambda_3)} \\ &+ h_3 e^{-L(\lambda_1+\lambda_3)} + h_4 e^{-L(\lambda_1-\lambda_3)} \end{aligned} \tag{38}$$

where, h_j $(j = 1, 2, 3, 4)$ consist of the elements in the eigenvector matrix details of which are omitted due to the space limitations. Considering the definition of the eigenvector matrix ($AV = \Lambda V$) and (38), it can be seen that $D(E_3^l)$ is a function of λ_j and tube parameters $(\hat{u}, k, l, L)$. In order to find the critical value ($\lambda^{\dagger\dagger}$) for the eigenvalues which makes $D(E_3^l) = 0$, the following nonlinear transformation is applied to (38).

$$Li\lambda_j = \arctan\left(\frac{\xi}{i\lambda_j}\right) \tag{39}$$

where ξ is the unknown parameter to be solved by substituting (39) into $D(E_3^l) = 0$. After solving ξ, the $\lambda^{\dagger\dagger}$ (that satisfies $D(E_3^l) = 0$) will be obtained:

$$\begin{aligned} Li\lambda^{\dagger\dagger} &= \arctan\left(\frac{k_1+k_2+k_3}{\left(\frac{1}{2}\sigma + \frac{1}{2}\sqrt{\sigma^2-\zeta}\right) i\lambda^{\dagger\dagger}}\right) \\ \sigma &= l_1(k_2+k_3) + l_2(k_1+k_3) + l_3(k_1+k_2) \\ \zeta &= (k_1+k_2+k_3)(k_1 l_2 l_3 + k_2 l_1 l_3 + k_3 l_1 l_2) \end{aligned} \tag{40}$$

Up to this point, the critical value ($\lambda^{\dagger\dagger}$) is achieved for a three-tube robot with straight parts. As discussed in (14)-(16), the following inequality can be obtained from (40):

$$L\|i\lambda^{\dagger\dagger}\| \geq \arctan\left(\frac{k_1+k_2+k_3}{\left(\frac{1}{2}\sigma + \frac{1}{2}\sqrt{\sigma^2-\zeta}\right)\|i\lambda^{\dagger\dagger}\|}\right) \tag{41}$$

Since ζ is a positive number, (41) results in:

$$L\|\lambda^{\dagger\dagger}\| \geq \arctan\left(\frac{k_1+k_2+k_3}{\sigma\|\lambda^{\dagger\dagger}\|}\right) \tag{42}$$

As mentioned before, adding straight parts to the robot design will change the boundary condition of the kinematics model while the characteristic equation remains the same. As a result, the conclusion achieved for λ_j in (35) is valid for a three-tube robot with straight parts. This means that the kinematics of a three-tube robot with straight parts will be unstable if the $\lambda^{\dagger\dagger}$ is within the bounds of the possible solutions for λ. In other words, considering (35), if the following holds, then the kinematics will be unstable:

$$\max(\sqrt{r_{mn}}) \geq \|\lambda^{\dagger\dagger}\| \tag{43}$$

Combining (42) and (43), it can be concluded that if the kinematics are unstable, we have:

$$L\max\left(\sqrt{r_{mn}}\right) \geq \arctan\left(\frac{k_1+k_2+k_3}{\sigma\max\left(\sqrt{r_{mn}}\right)}\right) \tag{44}$$

As a result, kinematic stability can be guaranteed if the tube parameters are chosen to satisfy the following stability condition for a three-tube robot with straight parts:

$$L\max\left(\sqrt{r_{mn}}\right) < \arctan\left(\frac{k_1+k_2+k_3}{\sigma\max\left(\sqrt{r_{mn}}\right)}\right) \tag{45}$$

The obtained stability condition is different from that for the two-tube case (18) due to the effect of the third tube. In (45), if the third tube stiffness is set to zero, then the stability condition reduces to the two-tube condition in (18).

C. Extension to Multiple Tubes

It is worth mentioning that the approach used in Section III can be used for robots with more than three tubes. It can be shown that the linearized model will always have a block anti-diagonal structure, which would result in a similar format for the characteristic polynomial corresponding to that in (32). So the conditions obtained in (37) can be extended for any number of tubes:

$$\max(L\sqrt{r_{mn}}) < \pi/2, \tag{46}$$

where $m, n = 1, 2, ..., p; m > n$, and p is the total number of tubes. For the robot with straight sections, when the kinematics are unstable, the critical values for the eigenvalues satisfy the relationship in (39), which would result in a similar inequality to that in (42). Following the technique developed in the previous subsection, it can be shown that the stability condition for the general case (multiple tubes with straight sections) is as follows:

$$\begin{aligned} L\max(\sqrt{r_{mn}}) &< \arctan\left(\frac{\sum_{m=1}^{p}(k_m)}{\sigma_p\max(\sqrt{r_{mn}}})\right) \\ \sigma_p &= (k_2+...+k_p)l_1 + (k_1+k_3+...+k_p)l_2 \\ &+ ... + (k_1+...+k_{p-1})l_p \end{aligned} \tag{47}$$

IV. Simulation Validation

In the first test, the stability of a two-tube robot with a straight portion is studied. For this robot, tube 1 (in Table I) is the inner tube and tube 2 is the outer one. The parameters of these two tubes, such as the length of the curved sections (L), pre-curvatures ($\hat{u}$), the stiffnesses (k), and Poisson's ratio (v) are defined as shown in Table I. The length of the straight part of tube 2 is equal to zero ($l_2 = 0$). In order to study the effect of l_1 (the straight part of tube 1) on kinematic stability, we need to determine at which value of l_1 the robot will be kinematically unstable. One way is to use the stability condition in (18). After some calculations, it can be shown that the robot is stable when l_1 is smaller than $0.051m$. Another way to achieve this result is to calculate the forward kinematics of the robot via simulation [11] when different values of l_1 are considered. As shown in Fig. 1, the tip position of the robot is calculated, when the inner tube rotates a full revolution and the outer tube remains stationary. This calculation was repeated many times when l_1 varies from 0 to $0.150m$. The simulation results shows that the robot is stable when $l_1 < 0.051m$ (blue curves), and critically stable when $l_1 = 0.051m$ (red curves). The purple curves have a discontinuous point in the tip Cartesian position during the continuous movement of the joint space

TABLE I
PARAMETERS OF CONCENTRIC-TUBE ROBOTS

	$L(m)$	$\hat{u}(m^{-1})$	$k\ (Nm^2)$	v
tube 1	0.157	1/0.120	0.040	0.3
tube 2	0.157	1/0.150	0.050	0.3
tube 3	0.157	1/0.180	0.060	0.3

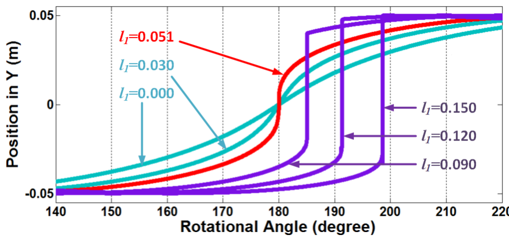

Fig. 1. Simulation results for a two-tube robot with straight sections. Y axis is the gravity direction in world frame.

values. This means that the tip of the robot suddenly jumps from one position to another in Cartesian domain. So the kinematics of the robot are unstable when $l_1 > 0.051m$. In conclusion, the simulation results are in an complete agreement with the derived stability condition. For a three-tube robot without any straight section, the stability condition becomes conservative, because the maximum value of λ_j in (35) is used for developing the stability condition. But when the three tubes have the same value of pre-curvatures, i.e., $\max(\sqrt{r_{mn}}) = \min(\sqrt{r_{mn}})$ in (33), the exact value of λ_j will be obtained (since the radius of the bound around λ_j converges to zero). In this specific situation, the stability condition is not conservative any more. A three-tube robot without straight sections is studied to verify this result. We assume that the inner, middle, and outer tubes of this robot have the same pre-curvature $\hat{u}_{123}$. The other parameters such as L, k, v are from tube 2. Using the stability condition in (37), it can be concluded that the robot will be stable if $\hat{u}_{123} < 1/0.114(m^{-1})$. In the simulation tests, the tip position of the robot is calculated when the inner tube rotates a full revolution and the other two tubes remain stationary. This procedure is repeated when $\hat{u}_{123}$ equals to a set of different values. As discussed earlier, the red line in Fig. 2 corresponds to the critically stable situation. So the kinematics are critically stable when $\hat{u}_{123} = 1/0.114(m^{-1})$, which agrees with the result in stability condition.

The last test is designed to validate the stability condition for a general three-tube robot which has three different pre-curvatures, stiffness and length for the straight parts. For this purpose, tube 1, tube 2 and tube 3 are chosen as the inner, middle and outer tubes of the robot, respectively. The straight parts of tube 2 and tube 3 were set to $l_2 = 0.010m, l_3 = 0$. Using the stability condition in (45), the robot is stable as long as $l_1 < 0.030m$. In simulation, the forward kinematics of the robot are calculated when tube 1 is rotated 360 degrees and the other two remain stationary. This calculation was repeated when l_1 equals a series of different values. As shown in the Fig. 3, compared to previous simulations, the robot did not show critical stability at $l_1 = 0.030m$, but at a higher value $l_1 = 0.048m$. This result shows that the stability

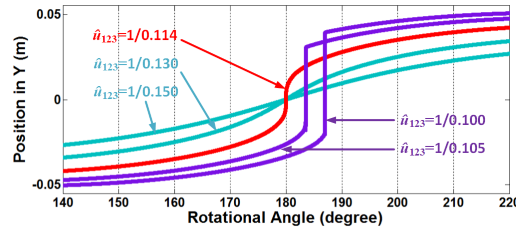

Fig. 2. Tip position of a three-tube robot without straight parts.

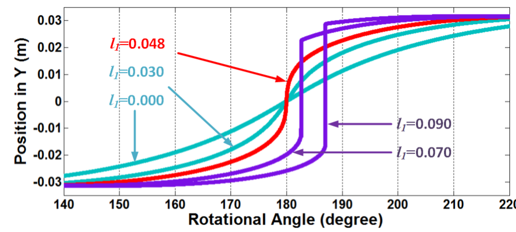

Fig. 3. Tip position of a three-tube robot with straight parts.

condition is conservative.

REFERENCES

[1] A. Gosline, N. V. Vasilyev, A. Veeramani, M. T. Wu, G. Schmitz, R. Chen, V. Arabagi, P. J. del Nido, P. E. Dupont, "Metal-MEMS tools for beating-heart tissue removal", *IEEE Int. Conf. Robotics and Automation*, pp. 1921-1936, 2012.

[2] N. V. Vasilyev, A. Gosline, E. Butler, N. Lang, P. Codd, H. Yamauchi, E. Feins, C. Folk, A. Cohen, R. Chen, P. J. del Nido, P. E. Dupont, "Percutaneous Steerable Robotic Tool Delivery Platform and Metal MEMS Device for Tissue Manipulation and Approximation: Initial Experience with Closure of Patent Foramen Ovale", *Circulation: Cardiovascular Interventions*, vol. 6, pp. 468-475, 2013.

[3] J. Burgner, P. J. Swaney, R. A. Lathrop, K. D. Weaver, and R. J. Webster III. "Debulking From Within: A Robotic Steerable Cannula for Intracerebral Hemorrhage Evacuation," *IEEE Trans. Biomed. Eng.*, vol. 60, no. 9, pp. 2567-2575, 2013.

[4] P. Dupont, J. Lock, B. Itkowitz, and E. Butler, "Design and Control of Concentric-tube Robots," *IEEE Trans. Robot.*, vol. 26, no. 2, pp. 209-225, 2010.

[5] R.J. Webster III, J.M. Romano, and N.J. Cowan, "Mechanics of Precurved-tube Continuum Robots," *IEEE Trans. Robot.*, vol. 25, no. 1, pp. 67-78, 2009.

[6] J. Lock and and P.E. Dupont, "Friction Modeling in Concentric Tube Robots," *In Proc. of IEEE Int. Conf. on Rob. Autom. (ICRA)*, 2011, pp. 1139-1146.

[7] D.C. Rucker, B.A. Jones, and R.J. Webster III, "A Geometrically Exact Model for Externally Loaded Concentric-tube Continuum Robots," *IEEE Trans. Robot.*, vol. 26, no. 5, pp. 769-780, 2010.

[8] R. Xu and R.V. Patel, "A Fast Torsionally Compliant Kinematic Model of Concentric-tube Robots," *In Proc. of 34th IEEE EMBS Annu. Int. Conf.*, 2012, pp. 904-907.

[9] Luis G. Torres and Ron Alterovitz, "Motion Planning for Concentric Tube Robots Using Mechanics-based Models," *In Proc. of IEEE/RSJ Int. Conf. on Intel. Rob. Sys. (IROS)*, 2011, pp. 5153-5159

[10] J. Burgner et al., "A Bimanual Teleoperated System for Endonasal Skull Base Surgery," *In Proc. of IEEE/RSJ Int. Conf. on Intel. Rob. Sys. (IROS)*, 2011, pp. 2517-2523.

[11] R. Xu, A. Asadian, A. Naidu, and R.V. Patel, "Position Control of Concentric-tube Continuum Robots using a Modified Jacobian-based Approach," *In Proc. of IEEE Int. Conf. on Rob. Autom. (ICRA)*, 2013, pp. 5793-5798.

[12] R. Xu, A. Asadian, S.F. Atashzar, and R.V. Patel, "Real-time Trajectory Tracking for Externally Loaded Concentric-tube Robots," *In Proc. of IEEE Int. Conf. on Rob. Autom. (ICRA)*, 2014. (in press)

[13] M. Mahvash and P.E. Dupont, "Stiffness Control of Surgical Continuum Manipulators," *IEEE Trans. Robot.*, vol. 27, no. 2, pp. 334-345, 2011.

[14] C. Bergeles and P.E. Dupont, "Planning stable paths for concentric tube robots," *In Proc. of IEEE/RSJ Int. Conf. on Intel. Rob. Sys. (IROS)*, 2013, pp. 3077-3082.